NASA/CR—2019–220236

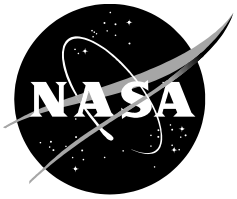

Airfoil Selection for Mars Rotor Applications

Witold J. F. Koning
Science and Technology Corporation
Ames Research Center, Moffett Field, California

July 2019

NASA STI Program ... in Profile

Since its founding, NASA has been dedicated to the advancement of aeronautics and space science. The NASA scientific and technical information (STI) program plays a key part in helping NASA maintain this important role.

The NASA STI program operates under the auspices of the Agency Chief Information Officer. It collects, organizes, provides for archiving, and disseminates NASA's STI. The NASA STI program provides access to the NTRS Registered and its public interface, the NASA Technical Reports Server, thus providing one of the largest collections of aeronautical and space science STI in the world. Results are published in both non-NASA channels and by NASA in the NASA STI Report Series, which includes the following report types:

- TECHNICAL PUBLICATION. Reports of completed research or a major significant phase of research that present the results of NASA Programs and include extensive data or theoretical analysis. Includes compilations of significant scientific and technical data and information deemed to be of continuing reference value. NASA counterpart of peer-reviewed formal professional papers but has less stringent limitations on manuscript length and extent of graphic presentations.

- TECHNICAL MEMORANDUM. Scientific and technical findings that are preliminary or of specialized interest, e.g., quick release reports, working papers, and bibliographies that contain minimal annotation. Does not contain extensive analysis.

- CONTRACTOR REPORT. Scientific and technical findings by NASA-sponsored contractors and grantees.

- CONFERENCE PUBLICATION. Collected papers from scientific and technical conferences, symposia, seminars, or other meetings sponsored or co-sponsored by NASA.

- SPECIAL PUBLICATION. Scientific, technical, or historical information from NASA programs, projects, and missions, often concerned with subjects having substantial public interest.

- TECHNICAL TRANSLATION. English-language translations of foreign scientific and technical material pertinent to NASA's mission.

Specialized services also include organizing and publishing research results, distributing specialized research announcements and feeds, providing information desk and personal search support, and enabling data exchange services.

For more information about the NASA STI program, see the following:

- Access the NASA STI program home page at http://www.sti.nasa.gov

- E-mail your question to help@sti.nasa.gov

- Phone the NASA STI Information Desk at 757-864-9658

- Write to:
  NASA STI Information Desk
  Mail Stop 148
  NASA Langley Research Center
  Hampton, VA 23681-2199

NASA/CR—2019–220236

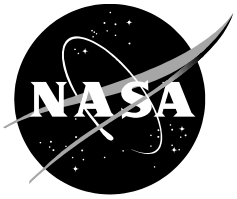

Airfoil Selection for Mars Rotor Applications

Witold J. F. Koning
Science and Technology Corporation
Ames Research Center, Moffett Field, California

National Aeronautics and
Space Administration

Ames Research Center
Moffett Field, CA 94035-1000

July 2019

ACKNOWLEDGMENTS

The author thanks Wayne Johnson, Larry Young, and Alan Wadcock for their helpful discussions while writing this paper.

Available from:

NASA STI Support Services
Mail Stop 148
NASA Langley Research Center
Hampton, VA 23681-2199
757-864-9658

National Technical Information Service
5301 Shawnee Road
Alexandria, VA 22312
webmail@ntis.gov
703-605-6000

This report is also available in electronic form at

http://ntrs.nasa.gov

TABLE OF CONTENTS

LIST OF FIGURES

LIST OF TABLES

AIRFOIL SELECTION FOR MARS ROTOR APPLICATIONS

Witold J. F. Koning[1]

Ames Research Center

INTRODUCTION

This paper provides an overview of design considerations for airfoil choices with rotor applications in the Martian atmosphere, at very low chord-based Reynolds number flows, around $Re_c = O\,(10^3\text{-}10^4)$. The low Reynolds number typical of rotorcraft operation in the Martian atmosphere reduces the rotor lifting force and efficiency, which is only partially compensated for by a lower gravity on Mars compared to Earth. Additionally, the low temperature and largely CO_2-based atmosphere of Mars compound the overall aerodynamic problem by resulting in a lower speed of sound, further constraining rotor operation in the Martian atmosphere by limiting the maximum rotor tip speed possible so as not to exceed an acceptable tip Mach number.

In light of the expected reduced rotor efficiency, evaluation of airfoils for compressible, low-Reynolds-number Mars rotor applications is key. Prior research on airfoil optimization and performance evaluation at low Reynolds numbers, especially in the compressible regime, is scarce and further investigation is needed. Specifically, the proposed goal stemming from this overview is to develop airfoils tailored to the unique demands of the second generation of Mars rotorcraft, i.e. the Mars Science Helicopter (MSH).

This research focuses on the airfoil performance at low Reynolds numbers and hopes to add to the work performed by Kroo et al.,[1] Kunz and Kroo,[2] Oyama and Fujii,[3] Anyoji et al.,[4–6] and others.

LOW-REYNOLDS-NUMBER AIRFOIL PERFORMANCE

McMasters and Henderson[7] provide a summary of attainable airfoil lift-to-drag ratios over a wide Reynolds number range in Figure 1. Results are collected from a wide variety of experiments, mostly with conventional airfoil geometries.

At the Reynolds number range under consideration, $Re_c = O\,(10^3\text{-}10^4)$, the boundary layer can be fully laminar up to the point of separation without subsequent (turbulent) flow reattachment or on-body transition.

[1] Science and Technology Corporation, NASA Research Park, Moffett Field, CA 94035.

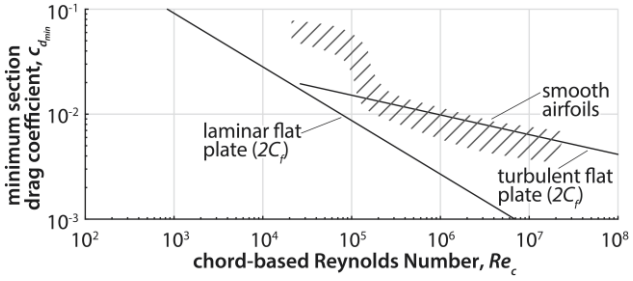

Figure 1. Maximum lift-to-drag ratio versus Reynolds number.[7]

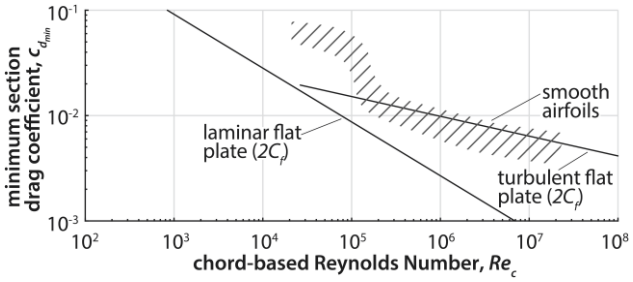

Figure 2. Minimum section drag coefficient versus Reynolds number.[7]

The Reynolds number effect on the minimum airfoil drag coefficient is presented in Figure 2. The flow state in absence of laminar-to-turbulent transition is called subcritical and derives its relatively low efficiency because of (a) the increased pressure drag component from early separation, and (b), to lesser extent, reduced lift due to an effective camber reduction.

The Reynolds number at which laminar flow over an airfoil begins to exhibit turbulent features (either due to on-body transition or turbulent reattachment) is called the critical Reynolds number. Reynolds numbers where turbulent transition always occurs before laminar separation, or during/after reattachment, are referred to as supercritical.

Finally, compressible flow—versus incompressible airfoil flow—is not well understood for low-Reynolds-number airfoils. Limited experimental and computational work in the literature—and performed previously by the author[8]—suggests that conventional airfoil geometries exhibit Mach-number sensitivities whereas cambered, flat-plate airfoils seem to be insensitive to Mach number.[4,6]

PERFORMANCE EVALUATION OF UNCONVENTIONAL AIRFOIL SHAPES

Overall airfoil performance changes with Reynolds number, especially the relatively poor performance (in terms of lift-to-drag ratio,[7] minimum section drag,[7,9] and maximum section lift[10]) up to $Re_c = O(10^5)$, serves as the main motivation for (unconventional) airfoil optimization in this regime. An example of the dramatic change in efficient airfoil shapes crossing this "barrier" becomes clear in the overview presented in Figure 3, by Lissaman.[11] It should be noted that the dragonfly and pigeon wing airfoil profiles are used in highly unsteady "flapping-wing" applications; their applicability to relatively steady "rotating-wing" operation is not necessarily ensured.

Figure 3. Various representative airfoil shapes versus Reynolds number.[11]

To identify future avenues for Mars rotor airfoil optimization research the following basic types of airfoil are examined: a conventional airfoil, a tripped/rough airfoil, a cambered plate, and a corrugated airfoil. Important factors in examining such airfoils are (a) airfoil sensitivity to operating conditions (with regard to laminar-turbulent transition), (b) possible hysteresis behavior with operating condition, and (c) relative technology readiness level of (unconventional) airfoil geometries and clear understanding of their aerodynamic behavior and analytic predictability.

Conventional Airfoil

A conventional airfoil is presumed to be relatively impractical for the transition region between subcritical and supercritical flow states. This "transition region" between the two flow states is difficult to analyze and reliably predict[12] because of a number of factors including the possible contribution of external influences such as free-stream turbulence (FST) levels, vibrations, and surface roughness on boundary layer transition.[13,14] Another factor is possible flow hysteresis (thought to stem mostly from highly unstable laminar separation bubble behavior with changing angle of attack).[12] Finally, unsteady laminar separation bubble features or transient boundary layer transition behavior, in turn, can give rise to unpredictable rotary-wing flight dynamics.[15] If the airfoils are operating only in subcritical mode, it is possible that cambered-plate airfoils can attain higher performance than conventional low-Reynolds-number airfoils, such as the Eppler 193, as shown in Figure 3.[7] The Jet Propulsion Laboratory (JPL) Mars Helicopter (MH) rotor airfoils are likely to operate fully subcritical in hover.[16] Previous work also indicates the competitiveness of cambered plates versus airfoils for rotor performance of the JPL Mars Helicopter technology demonstrator (MHTD).[8]

Tripped Airfoil

Conventional airfoils with a trip device (or an entirely "rough-surfaced" airfoil) can have lower Reynolds number sensitivity because of forcing or "fixing" transition.[7] The forcing of transition allows relatively good performance down to lower Reynolds numbers compared to smooth conventional airfoils.[17] However, ensuring a trip is functional—and, thereby, forcing transition—at very low Reynolds numbers is troublesome, and may be impossible below $Re_c \cong 30{,}000$. If transition cannot be guaranteed for the complete operational domain, the applicability of airfoil trips for rotary-wing application is unlikely because of the resulting unpredictable rotor performance and flight dynamic characteristics.

Cambered Plate

In contrast to a conventional airfoil, a cambered plate (also known as a circular-arc airfoil) is shown to be almost Reynolds number insensitive because of the resulting small, fixed leading-edge separation bubble that forms for all but a small (near zero) angle-of-attack range. The leading-edge flow separation will fix the separation bubble location and effectively limit Reynolds number sensitivity. This, in turn, reduces the possibility of hysteresis in lift, drag, and pitching moment as a function of angle of attack. It also reduces airfoil performance sensitivity to FST and other transient effects stemming from free-stream velocity variation and rotor blade pitching and flapping motion.

Prior research found that the cambered plate in this regime potentially outperforms conventional airfoils (in terms of minimum drag, maximum lift-to-drag ratio, and possibly maximum lift coefficient)[7,9,12,14,15,18,19] but the geometry variation for cambered plates in references is limited.[7,12,14,15,20,21]

Schmitz[12] lists the "advantageous cooperation of tangential incident flow at the leading edge at large angles of attack with the turbulence effect of the small nose radius", "the strongly concave underside, which shares significantly in the lift generation", "and the comparatively small camber of the airfoils top side, causing the flow to remain largely attached" as main reasons for the competitive performance of the cambered plate at these Reynolds numbers.

Corrugated Airfoil

The performance of a corrugated airfoil is potentially Reynolds number independent because of forcing fixed location(s) of separation. With the same reasoning applied to flat-plate airfoils, sensitivity to FST and other operating conditions is expected to be low. Research currently available for steady operation of corrugated airfoils is limited. Performance is likely to only be competitive at the lower end of the Reynolds number range under investigation, $Re_c \cong 1{,}000$.[21–23] It is also speculated that rotor blades incorporating corrugated airfoils might provide needed structural bending-moment and torsional stiffness (compared to the cambered-plate airfoils) in the inboard rotor region, where very low Reynolds numbers occur. Levy and Seifert investigated dragonfly airfoils, both using computational fluid dynamics (CFD) and experiments in steady free-stream flow, and found relatively promising performance figures in the range of $Re_c \cong 2{,}000$ to 8,000.[22]

The applicability of these various airfoil types in the Reynolds number range under consideration is assessed based on various published sources in the literature and summarized in Figure 4.

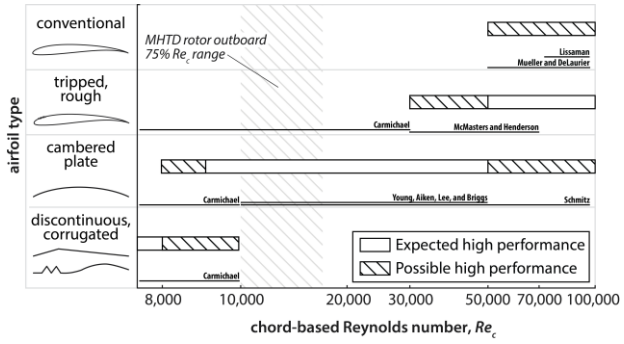

Figure 4. Performance of various airfoil shapes versus Reynolds number.[7,11,12,15,24,25]

Thickness Variation

The effect of a thickness distribution on the cambered plate and discontinuous type airfoils should be investigated. This could yield a higher structural bending-moment and torsional stiffness for a set of geometries that are inherently weak in that respect. Thickness distribution for the discontinuous or corrugated airfoils opens up a new domain—a family of polygonal airfoils. These can include triangular or diamond shape airfoils. Munday et al.[26] investigated a triangular airfoil in low-Reynolds-number compressible flow.

Table 1 provides an overview of the airfoil geometries and discusses their applicability in the current low-Reynolds-number regime.

Table 1. Overview of candidate airfoil shapes evaluated for $Re_c = O(10^3\text{-}10^4)$.

Airfoil Geometry	Re and FST Sensitivity	Hysteresis With Condition	Demonstrated Concept	Comments
Conventional airfoil	Large sensitivity possible	Hysteresis possible (laminar separation bubble induced)	If outside of critical Reynolds number region; used for small unmanned aerial vehicles (UAVs)	Can work reliably if Reynolds number is too low for boundary layer transition throughout operational regime like for the MHTD
Tripped airfoil, rough airfoil 	If transition is fixed, sensitivity is minimized	Hysteresis possible if bubble occurs before trip	Difficult to ensure trip works below *Re* = 30,000; uncertain at higher *Re* < 100,000	Transition needs to be guaranteed for all conditions otherwise unpredictable flight dynamics can ensue
Cambered plate, curved plate 	Leading-edge separation of large angle-of-attack range reduces sensitivity	Hysteresis less likely because of majority of operating conditions with leading-edge separation	Used for small UAVs or manned aerial vehicles (MAVs)	Possible stiffness issues due to low thickness/chord ratio (t/c)
Corrugated airfoil 	Separation at corrugation features likely to reduce sensitivity	Hysteresis less likely because of separation at corrugation features	No rotary-wing experiments using corrugated airfoils known	Performance only competitive at lower *Re* < 10,000
Polygonal airfoil 	Separation at corrugation features likely to reduce sensitivity	Hysteresis less likely because of separation at corrugation features	No rotary-wing experiments using polygonal airfoils known	Possible mediation of stiffness issues due to increased t/c compared to corrugated airfoil

SHAPE OPTIMIZATION EFFORTS

Figure 4 shows that the geometry of the cambered-plate-type airfoil seems to be a logical avenue for further research, as its optimal aerodynamic performance is roughly at the expected rotor chord-based Reynolds number range for Mars rotor applications. The geometry variation for cambered plates in literature is limited,[7,12,14,15,20,21] implying cambered-plate airfoil performance optimization for plates (wherein nonlinear camber lines, chordwise plate thickness distributions, and even local corrugation features can be examined) could yield performance improvements over the "simple cambered plate" often presented in literature. The Reynolds number influence on optimal shape and high Mach/compressibility effects on optimal performance (for desired cruise speeds) can be subsequently evaluated.

Airfoil geometry optimization can, unfortunately, produce a solution space with various local extremes, making gradient-based optimization techniques less applicable because of the criticality of finding an appropriate starting location. Alternatively, a genetic algorithm for airfoil optimization allows for a potentially more robust exploration of the solution space for a wide variety of airfoil shapes, providing greater insight into the aerodynamic performance of various airfoil shapes.

A custom airfoil design genetic algorithm has been written in Python and is able to optimize airfoil shapes using a preset number of design variables. The algorithm performs OVERFLOW grid generation and case execution, variation of airfoil geometry within set constraints, and post processing of OVERFLOW output. The algorithm has been demonstrated on the NASA Ames Pleiades supercomputer, and can queue run cases on different nodes and central processing units (CPUs) depending on the population size being evaluated. Currently the algorithm is operating as a single-objective optimization (SOO) at fixed alpha or lift coefficient. The optimized airfoils can be used to generate airfoil C81 input decks to evaluate rotor performance using comprehensive rotorcraft analyses as done previously for the JPL MHTD development effort.[27]

Future enhancement of the genetic algorithm airfoil optimization will include the ability to perform multi-objective optimization (MOO), evaluation of rotor blade thickness/stiffness spanwise distributions, and ultimately, coupling to the Comprehensive Analytical Model of Rotorcraft Aerodynamics and Dynamics (CAMRAD) comprehensive rotor analysis software tool.

The progress is aimed at increasing the understanding of low-Reynolds-number airfoil performance and developing airfoils tailored to the unique demands of second generation Mars rotorcraft, i.e. the MSH.

Care must be taken in airfoil selection; direct consequences on various rotor design parameters such as blade stiffness and structural frequencies, blade chordwise center-of-gravity placement, and possible aeroelastic effects such as blade flutter or "live twist" must be considered.

REFERENCES

1 Kroo, I., Prinz, F., Shantz, M., Kunz, P., Fay, G., Cheng, S., Fabian, T., and Partridge, C.: The Mesicopter: A Miniature Rotorcraft Concept Phase II Interim Report, *Stanford University*, Palo Alto, CA, 2000.

2 Kunz, P. J., and Kroo, I.: Analysis and Design of Airfoils for Use at Ultra-Low Reynolds Numbers, *Fixed and Flapping Wing Aerodynamics for Micro Air Vehicle Applications*, vol. 195, 2001, pp. 35–59.

3 Oyama, A., and Fujii, K.: A Study on Airfoil Design for Future Mars Airplane, *44th AIAA Aerospace Sciences Meeting and Exhibit*, Reno, NV, 2006, p. 1484.

4 Anyoji, M., Nose, K., Ida, S., Numata, D., Nagai, H., and Asai, K.: Low Reynolds Number Airfoil Testing in a Mars Wind Tunnel, *40th Fluid Dynamics Conference and Exhibit*, Chicago, IL, 2010, p. 4627.

5 Anyoji, M., Nonomura, T., Aono, H., Oyama, A., Fujii, K., Nagai, H., and Asai, K.: Computational and Experimental Analysis of a High-Performance Airfoil Under Low-Reynolds-Number Flow Condition, *Journal of Aircraft*, vol. 51, 2014, pp. 1864–1872.

6 Anyoji, M., Numata, D., Nagai, H., and Asai, K.: Effects of Mach Number and Specific Heat Ratio on Low-Reynolds-Number Airfoil Flows, *AIAA Journal*, vol. 53, Oct. 2014, pp. 1640–1654.

7 McMasters, J., and Henderson, M.: Low-Speed Single-Element Airfoil Synthesis, *Technical Soaring*, vol. 6, 1980, pp. 1–21.

8 Koning, W. J. F., Romander, E. A., and Johnson, W.: Low Reynolds Number Airfoil Evaluation for the Mars Helicopter Rotor, *AHS International 74th Annual Forum & Technology Display*, Phoenix, AZ, 2018.

9 Hoerner, S. F.: *Fluid-Dynamic Drag: Practical Information on Aerodynamic Drag and Hydrodynamic Resistance*, Hoerner Fluid Dynamics, 1965.

10 Hoerner, S. F., and Borst, H. V.: *Fluid-Dynamic Lift: Practical Information on Aerodynamic and Hydrodynamic Lift*, Hoerner Fluid Dynamics, 1985.

11 Lissaman, P. B. S.: Low-Reynolds-Number Airfoils, *Annual Review of Fluid Mechanics*, vol. 15, 1983, pp. 223–239.

12 Schmitz, F. W.: *Aerodynamics of the Model Airplane. Part 1 - Airfoil Measurements*, Huntsville, AL, 1967.

13 Van Ingen, J.: The eN Method for Transition Prediction. Historical Review of Work at TU Delft, *38th Fluid Dynamics Conference and Exhibit*, 2008, Seattle, WA, p. 3830.

14 Laitone, E. V.: Wind Tunnel Tests of Wings at Reynolds Numbers Below 70 000, *Experiments in Fluids*, vol. 23, Nov. 1997, pp. 405–409.

15 Carmichael, B. H.: *Low Reynolds Number Airfoil Survey, Volume 1*, Capistrano Beach, CA, 1981.

16 Koning, W. J. F., Johnson, W., and Allan, B. G.: Generation of Mars Helicopter Rotor Model for Comprehensive Analyses, *AHS Aeromechanics Design for Transformative Vertical Flight*, San Francisco, CA, 2018.

17 McMasters, J. H., and Henderson, M. L.: Low-Speed Single-Element Airfoil Synthesis, *Third International Symposium on the Science and Technology of Low Speed and Motorless Flight*, Seattle, WA, 1979, pp. 19, 23.

18 McArthur, J.: *Aerodynamics of Wings at Low Reynolds Numbers: Boundary Layer Separation and Reattachment*, University of Southern California, Los Angeles, CA, 2008.

19 Winslow, J., Otsuka, H., Govindarajan, B., and Chopra, I.: Basic Understanding of Airfoil Characteristics at Low Reynolds Numbers (104–105), *Journal of Aircraft*, Dec. 2017, pp. 1–12.

20 Wazzan, A. R., Okamura, T. T., and Smith, A. M. O.: *Spatial and Temporal Stability Charts for the Falkner-Skan Boundary-Layer Profiles*, 1968.

21 Okamoto, M., Yasuda, K., and Azuma, A.: Aerodynamic Characteristics of the Wings and Body of a Dragonfly, *The Journal of Experimental Biology*, vol. 199, Feb. 1996, p. 281 LP-294.

22 Levy, D.-E., and Seifert, A.: Simplified Dragonfly Airfoil Aerodynamics at Reynolds Numbers Below 8000, *Physics of Fluids*, vol. 21, 2009, p. 71901.

23 Kesel, A. B.: Aerodynamic Characteristics of Dragonfly Wing Sections Compared With Technical Aerofoils, *Journal of Experimental Biology*, vol. 203, 2000, pp. 3125–3135.

24 Mueller, T. J., and DeLaurier, J. D.: Aerodynamics of Small Vehicles, *Annual Review of Fluid Mechanics*, vol. 35, Jan. 2003, pp. 89–111.

25 Young, L. A., Aiken, E., Lee, P., and Briggs, G.: Mars Rotorcraft: Possibilities, Limitations, and Implications for Human/Robotic Exploration, *IEEE Aerospace Conference*, Big Sky, MT, 2005.

26 Munday, P. M., Taira, K., Suwa, T., Numata, D., and Asai, K.: Nonlinear Lift on a Triangular Airfoil in Low-Reynolds-Number Compressible Flow, *Journal of Aircraft*, vol. 52, 2014, pp. 924–931.

27 Koning, W. J. F., Johnson, W., and Grip, H. F.: Improved Mars Helicopter Aerodynamic Rotor Model for Comprehensive Analyses, *44th European Rotorcraft Forum*, Delft, the Netherlands, 2018.